# Chapter 5

## *Light Emitting Nanocrystalline Silicon Nano-Structures Grown by Layer-by-Layer Deposition*

## 5.1 Introduction

The results in Chapter 4 established that the hydrogenated silicon (Si:H) films deposited by layer-by-layer (LBL) deposition are more crystalline compared to the films deposited by continuous deposition (CD). The films deposited on crystalline silicon (c-Si) substrates were also shown to be more crystalline. The objective of the work done in this chapter is to study the photoluminescence (PL) emission properties of the mixed phases of nc-Si:H films grown by LBL deposition technique on c-Si substrates using plasma enhanced chemical vapour deposition (PECVD). From the morphology and structural properties of the films an attempt will be made to suggest the growth kinetics and structure of these films, and relate it to the PL emission properties. Since PL emission properties are strongly influenced by the crystalline properties of the material, only materials showing evidence of high crystallinity are studied in this chapter. From the analysis of the results in the previous chapter, films deposited on c-Si substrates prepared at different rf powers and substrate temperatures are selected for this study. The structural properties investigation will be concentrated on the morphology, crystallinity, crystallite size and silicon-oxygen bonding properties of this material in relation to the deposition parameters will be studied. The silicon-oxygen bonding properties will be extracted from the FTIR spectra of the films presented in Chapter 4. Micro-Raman scattering spectroscopy, field emission scanning electron microscopy (FESEM), high resolution transmission electron microscope (HRTEM) and Micro-Photoluminescence (PL) spectroscopy characterization techniques will be used to characterize samples deposited at the same substrate temperatures and rf powers studied in Chapter 4.

## 5.2 Micro-Raman Scattering Spectroscopy

The Micro-Raman scattering spectroscopy is a fast, non-destructive and powerful characterization technique that is usually employed to verify and characterize the crystalline volume fraction in mixed phases of hydrogenated amorphous/nanocrystalline silicon (a/nc-Si:H) films. The Micro-Raman scattering spectra of the films in this work were obtained using Horiba Jobin Yvon 800 UV Micro-Raman Spectrometer with CCD detector. The laser power was fixed at 20 mW. The excitation wavelength used was 514.5 nm $Ar^+$ laser and the laser was focused onto a spot of 1 um in diameter to collect the backscattered light for the measurement. The Raman spectra of a-Si:H films exhibit a broad peak 480 $cm^{-1}$ corresponding to the transverse optical (TO) Si-Si mode. On the other hand, films of mixed phases of a/nc-Si:H exhibit an additional Raman peak at 520 $cm^{-1}$ related to the TO mode of c-Si (Marinov and Zotov, 1997; Ehbrecht *et al.*, 1997; Furukawa and Miyasato, 1988; Charvet *et al.*, 2004). XRD measurements were done to study evidence of crystallinity in these films and were presented and discussed in the previous chapter. Although Micro-Raman scattering spectroscopy also studies evidence of crystallinity in films, it has additional advantage of being able to focus on position of interest for measurement and also quantify the crystalline volume fraction of the point of measurement. In this work, the LBL deposited films on c-Si emit photoluminescence (PL) only in regions of the films where aggregates of Si grains features were observed. Since the objective of this part of this work is to relate the structure and morphology of these Si grains to the PL properties of the films, the Raman scattering spectroscopy measurement focused on the location of these grains is considered to be more accurate for this purpose. The scanning electron microscopy (SEM) and transmission electron microscopy (TEM) measurements are also focused on these Si grains for an accurate interpretation of the results. Figure 5.1 shows the optical microscope image of the film deposited by LBL

deposition technique at rf power of 60 W. The magnification of the image is 100× and the selected area is focused for Raman mapping. The Micro-Raman scattering image taken at the selected area where the Si grains aggregates on the LBL film is observed and a single spectrum of highlighted area for the films deposited by LBL deposition technique is shown in Figure 5.2.

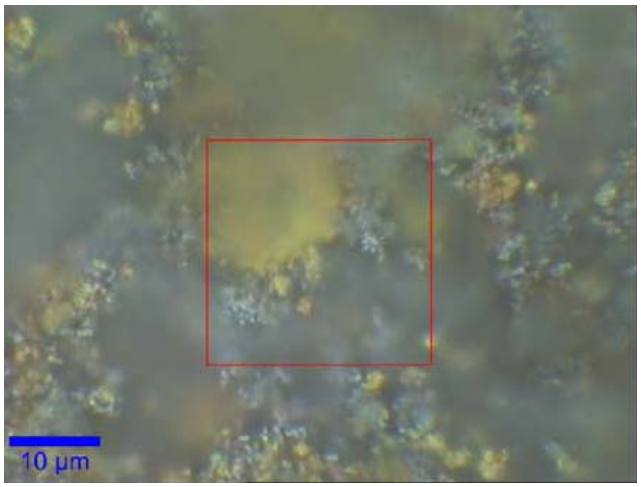


Figure 5.1: Optical microscope image of the films deposited by LBL deposition technique at rf power of 60 W.

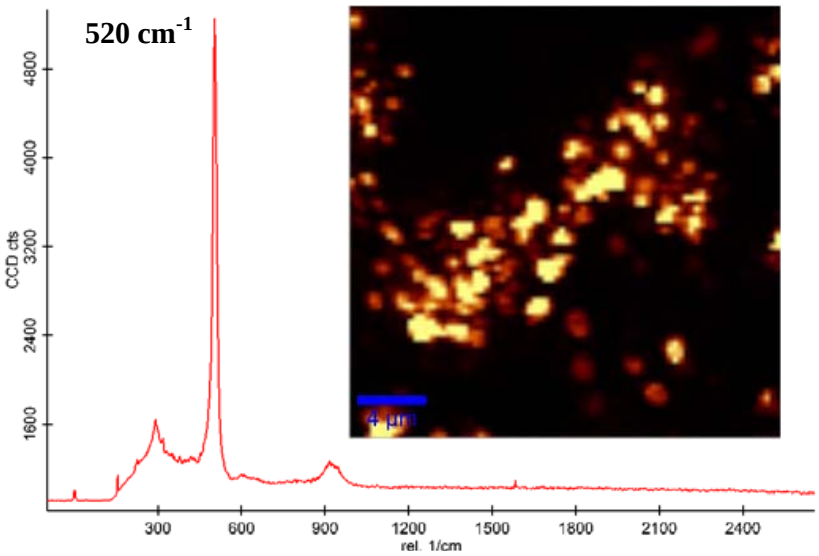


Figure 5.2: Micro-Raman scattering image and single spectrum of highlighted area for the films deposited by LBL deposition technique at rf power of 60 W (scan area = 25µm×25µm).

*5.2.1 Raman Scattering Spectra*

Figure 5.3 shows the Micro-Raman scattering spectra of the films deposited by LBL deposition technique at different rf powers. The Raman spectrum of the film prepared at 20 W exhibits its amorphous structure by the characteristic broad peak at 485 $cm^{-1}$. This peak width decreases and is shifted to higher wavenumber at 494 and 495 $cm^{-1}$ for the films prepared at 60 and 80 W respectively. This is an indication of increase in the structural order in the film. The narrowing and shifting of this characteristic Raman peak for a-Si towards 520 $cm^{-1}$ which is related to the TO mode of c-Si indicate the presence of clusters of Si nano-crystallites surrounded by grain boundaries embedded in amorphous matrix (Jeon *et al.*, 2005; Modreanu *et al.*, 2005; Wang *et al.*, 2005). The large shift in the peak position away from the 520 $cm^{-1}$ peak is attributed to high residual stress of Si-Si network in the film and also the extremely small size of the Si nano-crystallites clusters. The film prepared at rf power of 100 W shows a broad amorphous Si peak centred at 480 $cm^{-1}$ with small protrusion of crystalline Si peak at 518 $cm^{-1}$. This film is of mixed phases of amorphous and crystalline components but the Si nano-crystallites clusters are larger in size as a result of lower residual stress of the Si-Si network as indicated by the small shift of the crystalline Si peak away from 520 $cm^{-1}$. This is consistent with results from other work on nc-Si:H deposited by conventional rf PECVD where higher rf power has been reported to increase crystallite size (Dinh *et al.*, 1996). In LBL process, the more energetic hydrogen atoms reaching the substrates during the hydrogen plasma treatment at high rf power create nucleation sites for growth of Si nano-crystallites clusters and the presence of more energetic hydrogen radicals at the growth sites during the deposition process further enhance the growth of large Si nano-crystalline grains. However, depletion of $SiH_4$ molecules and high bomnardment effects at this rf power also result in the large volume of amorphous component in the film.

The Micro-Raman scattering spectra for the films deposited at different substrate temperatures are shown in Figure 5.4. All the Raman spectra of these films show sharp crystalline peaks at positions in the range of 490 $cm^{-1}$ to 504 $cm^{-1}$. The Raman peaks appear to shift away from the c-Si peak at 520 $cm^{-1}$ with increase in substrate temperature suggesting increase in residual stress of the Si-Si network and decrease in crystallite size.

*5.2.2 Crystalline Volume Fraction from Raman Spectra of Films*

The asymmetric Raman peaks obtained for most the films implies that these peaks are multi-component peaks. The Raman spectra of the films prepared at different rf powers and substrate temperatures with obvious multi-component peaks are deconvoluted into three Gaussian components using Origin Pro version 8.1, as shown in Figures 5.5 and 5.6 respectively. These Gaussian components represent the amorphous, intermediate and crystalline components which characteristics of the Raman spectra of nc-Si:H (Liu *et al.*, 1998; Sato and Hirakuri, 2005). The crystalline volume fraction, $X_C$ and the crystallite size, $d$ were determined follow the relations as described in Section 3.3.4. The $\Delta\omega$ in the relation is referred to $\omega_{c-Si} - \omega_{nc-Si}$, where $\omega_{c\text{-}Si}$ and $\omega_{nc\text{-}Si}$ are the wavenumber of TO phonon of c-Si and Si nano-crystallite respectively.

In this work, after deconvolution, the peak for all the films are located at around 480 $cm^{-1}$ which is usually associated to the amorphous Si component. Increase in structural order in the amorphous Si matrix is indicated by the shifting of this a-Si Raman peak towards 490 $cm^{-1}$ (Choi *et al.*, 1998). The Raman peak located in the range between 490 $cm^{-1}$ to 504 $cm^{-1}$ is associated with grain boundaries (Liu *et al.*, 1998; Sato and Hirakuri, 2005) or region with very small crystallites of size less than 3 nm surrounded by amorphous grain boundaries (Bi *et al.*, 2006). With respect to this, the integrated intensities representing the crystalline component, ($I_{500} + I_{520}$) of the films in

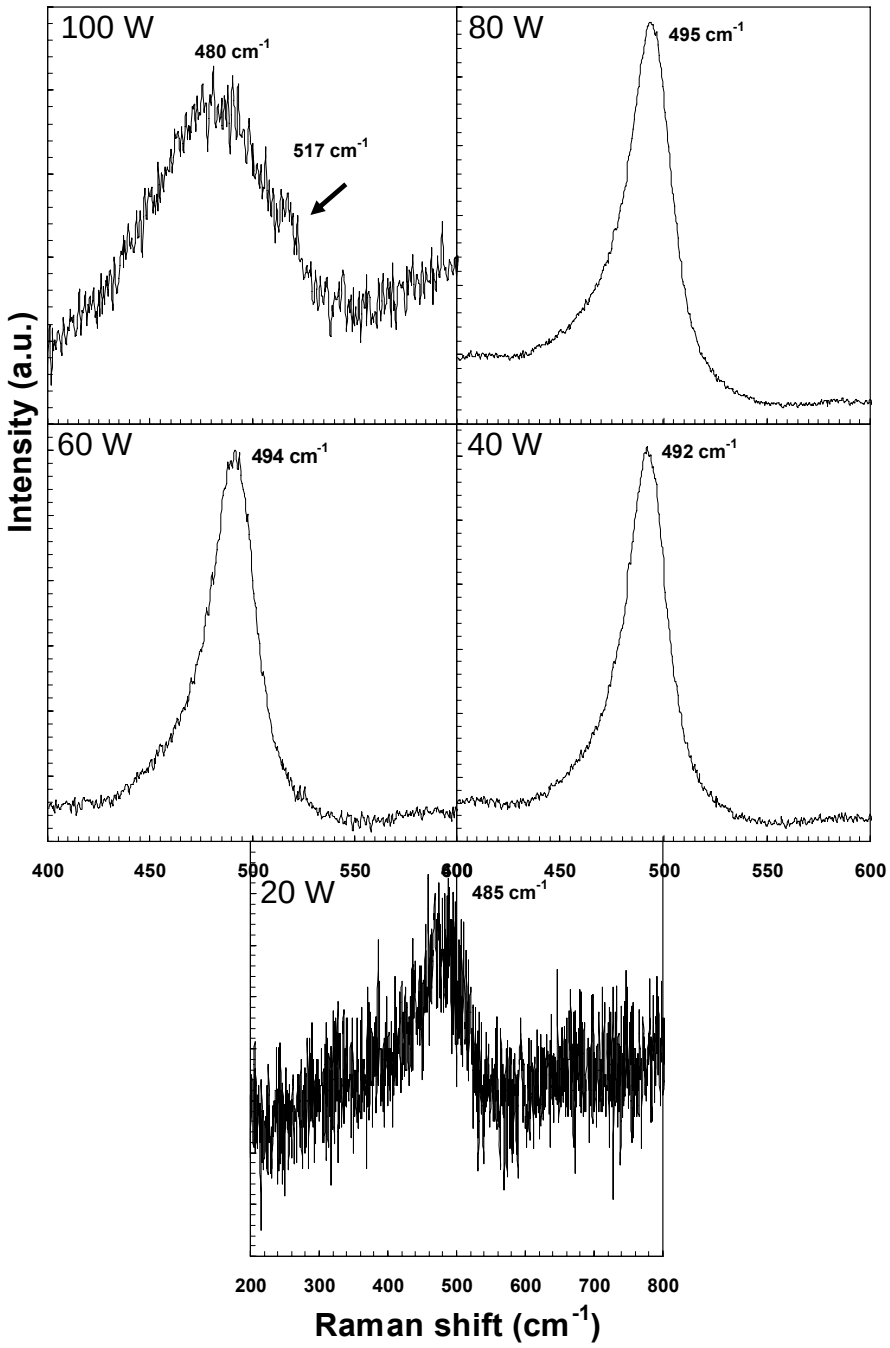


Figure 5.3: Micro-Raman scattering spectra of the films deposited by LBL deposition technique at different rf powers.

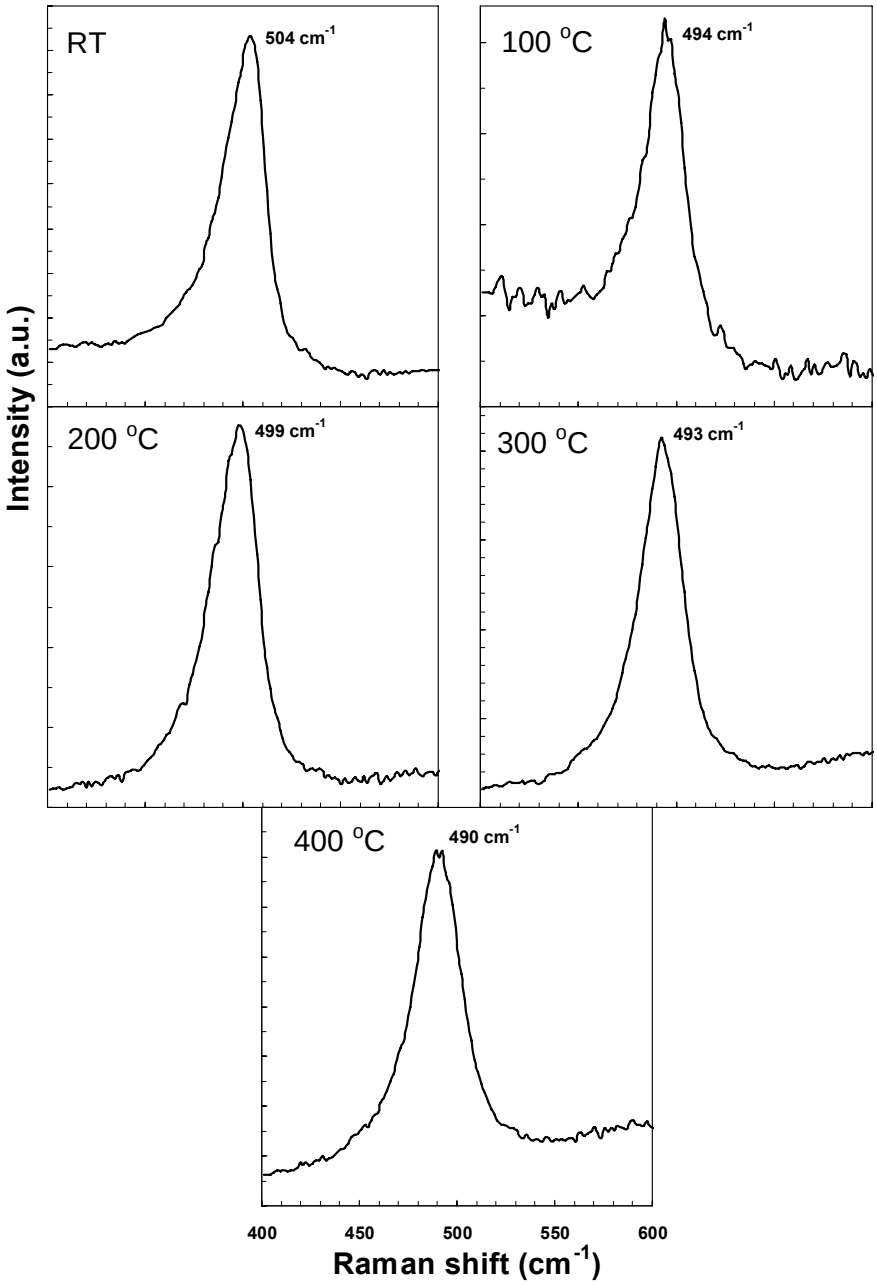


Figure 5.4: Micro-Raman scattering spectra of the films deposited by LBL deposition technique at different substrate temperatures.

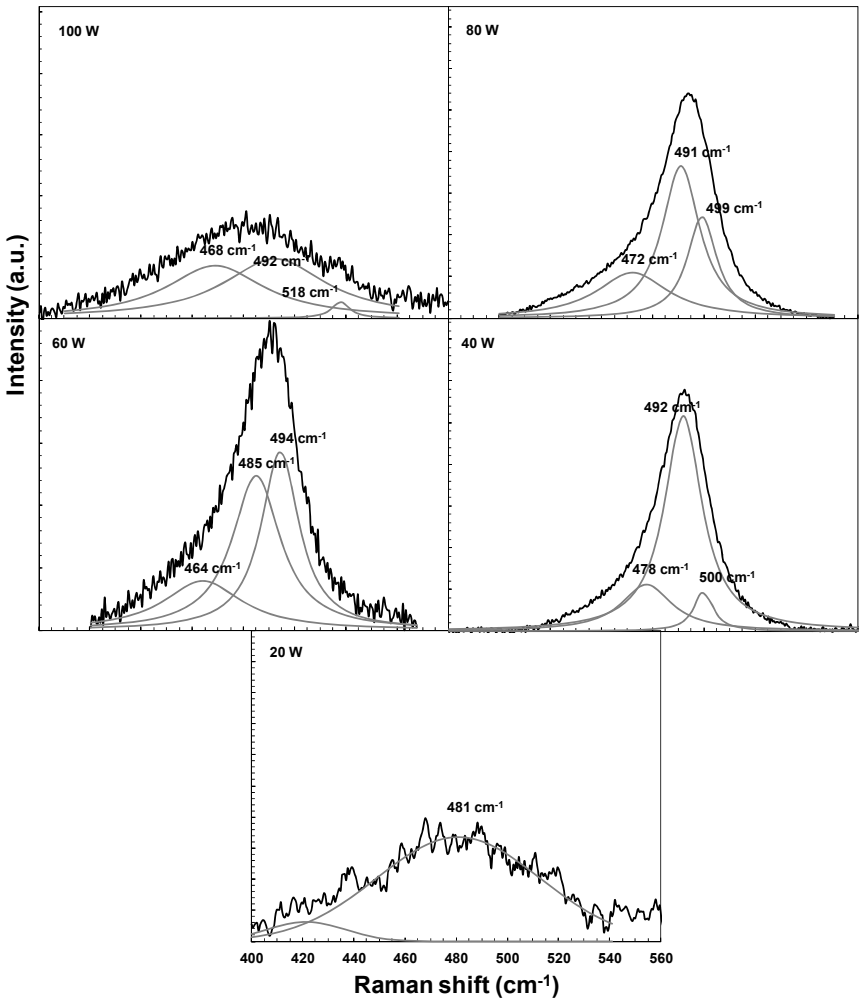


Figure 5.5: Gaussian deconvolution of Raman peak at around 500 $cm^{-1}$ for the films deposited at different rf powers. The line shapes of the three satellite components are labelled in the figure.

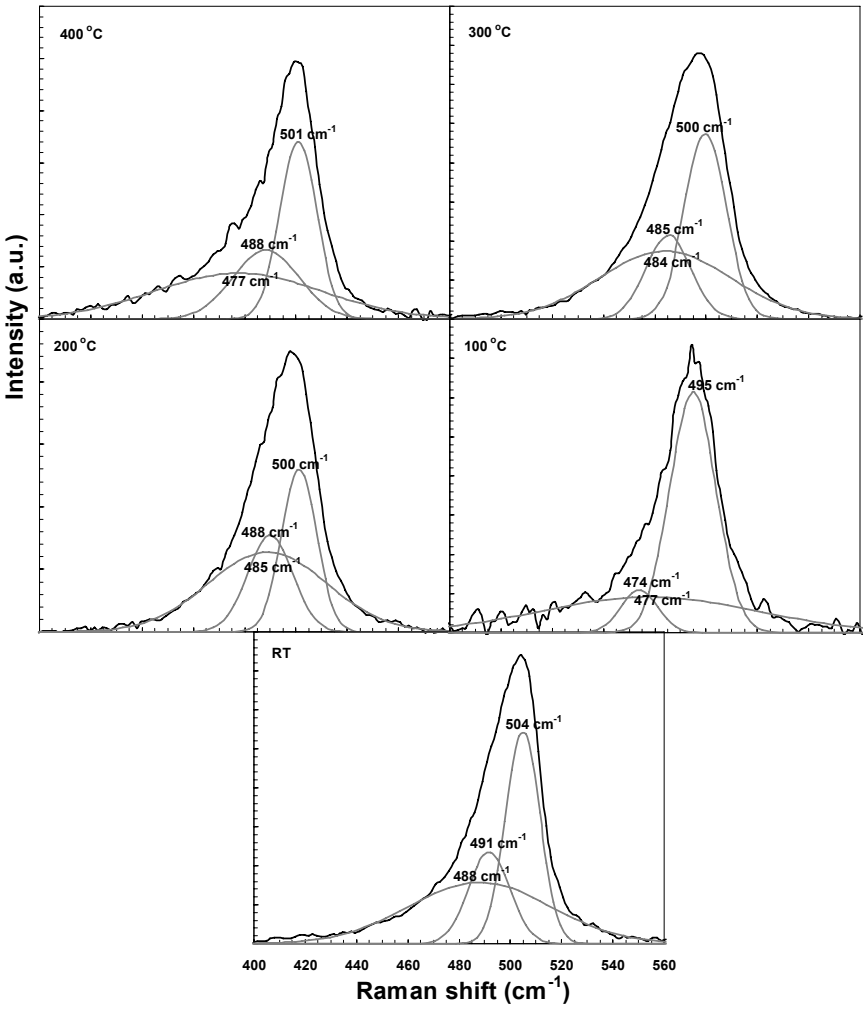


Figure 5.6: Gaussian deconvolution of Raman peak at around 500 $cm^{-1}$ of the films deposited at different substrate temperatures. The line shapes of the three satellite components are labelled in the figure.

this work is represent by the integrated intensities of deconvoluted peaks above 490 $cm^{-1}$. The values of $X_C$ for the LBL deposited on c-Si substrate are tabulated in Table 5.1.

Table 5.1: Calculated crystalline volume fraction, $X_C$ and crystallite size of the LBL films deposited different rf powers and substrate temperatures, $T_s$.

| | Deposition Parameters | Crystalline volume fraction, $X_C$ (±6%) *on c-Si* | Crystallite Size (±0.2 nm) |
|---|---|---|---|
| Fixed $T_s$ = 300°C, $R$ = 20 sccm, varied rf power | 20 W | - | - |
| | 40 W | 41 | 2.1 |
| | 60 W | 41 | 1.8 |
| | 80 W | 44 | 2.0 |
| | 100 W | 25 | 5.0 |
| Fixed $R$ = 20 sccm, rf power = 40 W, varied $T_s$ | RT | 40 | 2.3 |
| | 100°C | 54 | 1.9 |
| | 200°C | 45 | 2.1 |
| | 300°C | 38 | 2.1 |
| | 400°C | 35 | 2.1 |

Table 5.1 tabulates the crystalline volume fraction and the crystallite sizes as calculated from the Raman spectra of the samples. The crystalline volume fraction, $X_C$ of the Si grains on the LBL films deposited on c-Si substrate increases from 41 % for the film deposited at rf power of 40 W to 44 % for the film deposited at rf power of 80 W but decreases to 25 % for film prepared at rf power of 100 W. The crystallinity of these films is contributed by very small Si crystallites of size less than 3 nm as indicated by the Raman peak position. The depletion of $SiH_4$ molecules and increase in ion bombardment effects during deposition at the highest rf power contribute to the decrease in $X_C$ in the film. The low rf power of 20 W reduces the hydrogen etching effect during the hydrogen plasma treatments of the LBL deposition process thus resulting in an amorphous film structure. Increasing $T_s$ to 100°C increases the $X_C$ of the deposited film to 54 % but further increase in $T_s$ resulted in deterioration in the crystallinity in the film structure. This may be due to increase in the size of the clusters of Si nano-crystallites at higher temperature. Increase in $T_s$ may result in increase in

agglomeration of the crystallites resulting in the increase in the number and size of voids in between the clusters which are filled with amorphous Si phase. This will be confirmed later from the SEM results. The crystallite sizes appear to be insensitive to rf power and substrate temperature and the sizes in the order of 1.8 to 2.3 nm. This crystallite sizes will be compared to the size determined from the XRD diffraction peaks of the films and analysis will be done to suggest the structure of the sample deposited by LBL deposition.

### 5.3 Analysis on Field Emission Scanning Electron Microscope Images

The field emission scanning electron microscope (FESEM) images in this work were obtained using FESEM model FEi Quanta 200 at 20 kV. The surface morphologies of the films deposited at different rf powers as observed by FESEM images in Figure 5.7. For the films deposited at rf power of 20 W, different sizes of Si grain aggregates are randomly distributed on the irradiated area of the film. These Si grains are clusters of strained Si-Si bonds separated by region of homogeneous hydrogenated amorphous Si phases. For the film prepared at rf power of 40 W, uniformly distributed, clusters of smaller sized grains are distributed uniformly over the scanned area of the film. Further increase in rf power to 60 W showed a further decrease in grain size but larger clusters of grains are observed. The Raman spectroscopy results showed that the 40 and 60 W films consist of clusters of Si grains with 41 % of Si nano-crystallites separated by an amorphous grain boundary. The grain size in the film prepared at rf power of 80 W increase and the clusters are loosely packed together producing large voids in between the clusters. This is due to the agglomeration of Si grains during the deposition process at this rf power. Smaller sized grains are also observed around the larger sized grains. The crystalline phase in the grains also increases slightly to 44 %. The surface morphology of the film prepared at rf

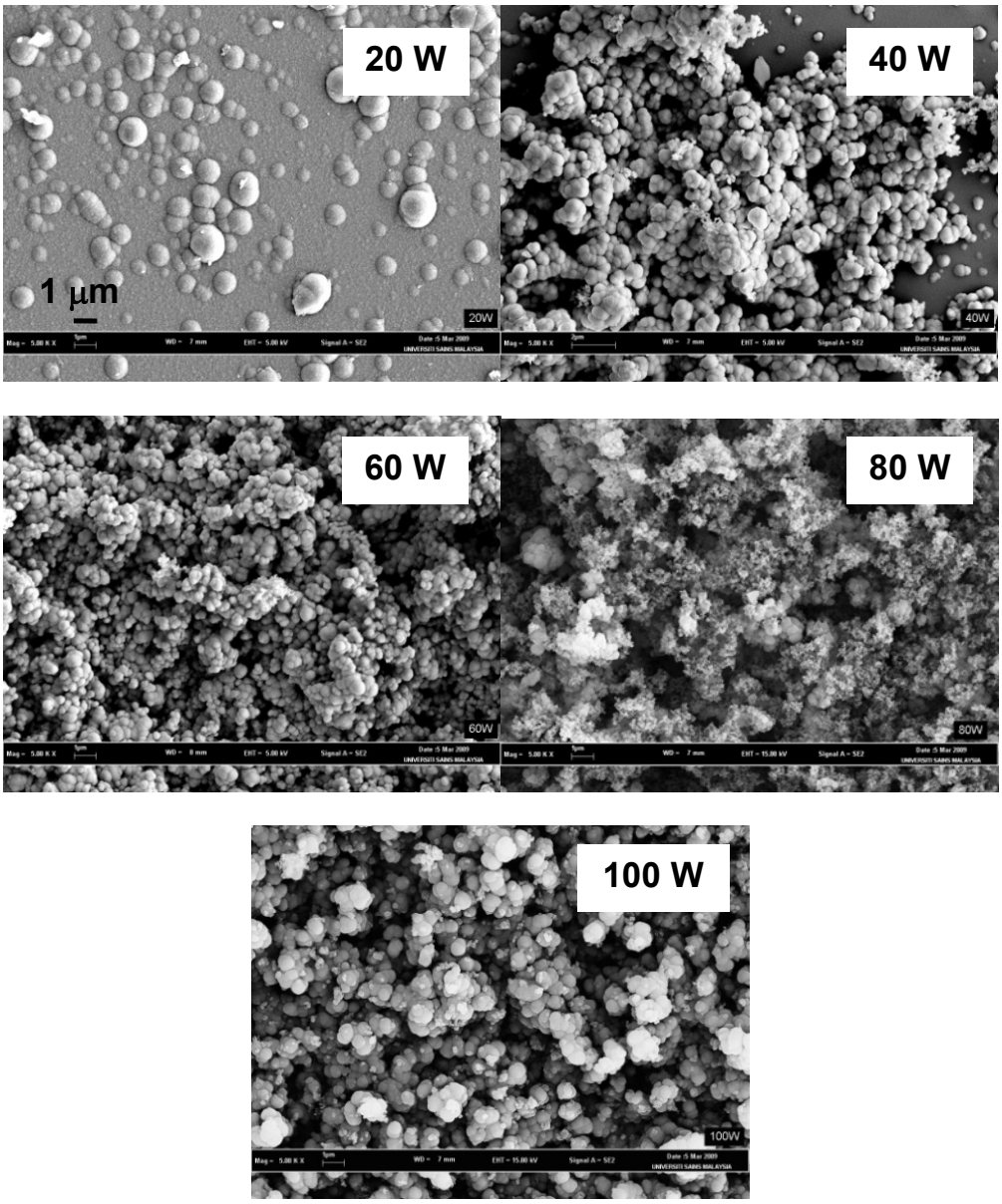


Figure 5.7: FESEM images of the films deposited by LBL deposition technique at different rf powers.

power of 100 W shows the formation of uniformly larger sized Si grains evenly distributed on the surface of the film. These larger grains actually are mixed phases of amorphous and crystalline phase with the crystalline phase volume fraction of only 25 % as indicated from the analysis of the Raman spectrum of the film.

The grain size distribution in the films is measured from the FESEM images of the films. This quantitative analysis is only performed for the films with Si grains visible within the magnification of the FESEM images. The existence of very small

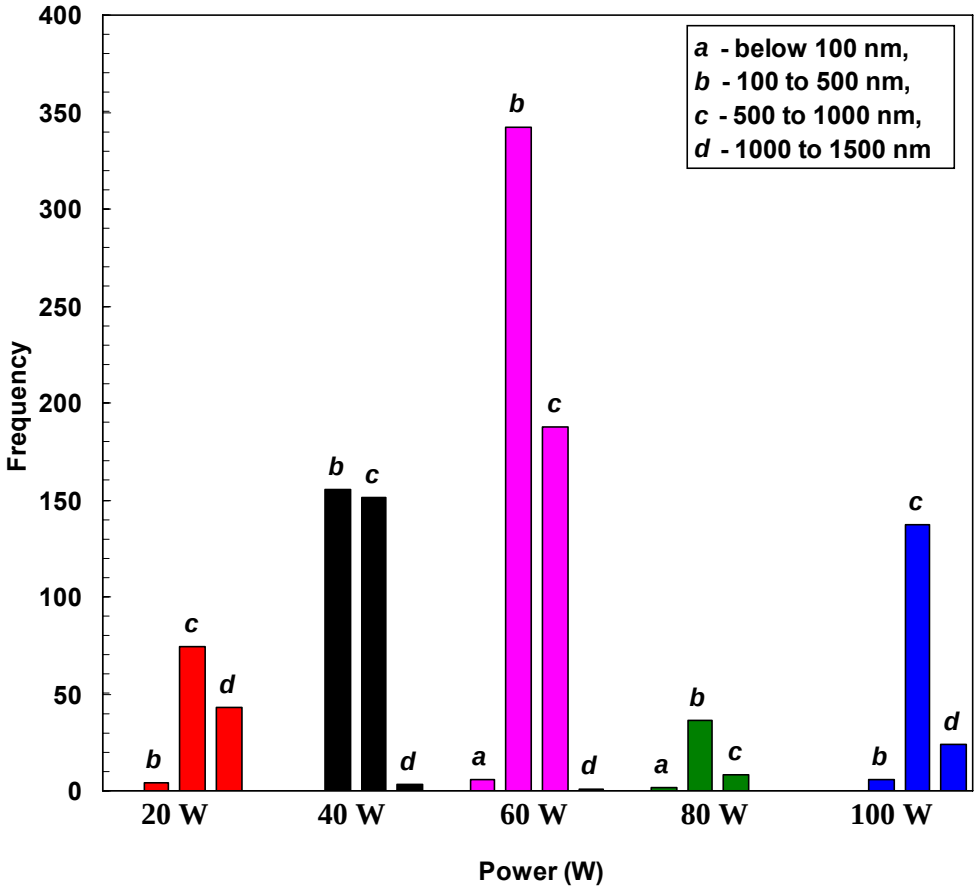


Figure 5.8: Grain size distribution plot for the LBL Si:H films deposited at different rf powers.

sized grains present in the image is not included from this grain size distribution plots as the accuracy of the measurement is too low. It should be noted here that these grains consists of either totally amorphous Si grains or mixed phases of a/nc-Si:H grains as shown by the Raman scattering spectroscopy results in the previous section.

The grain size distribution plots for the films deposited at different rf power as measured from FESEM images are presented in Figure 5.8. The films deposited at rf powers of 20 and 100 W show comparatively much larger grains with diameter above 1 μm. However, the Raman results show that the grains in the 20 W films are totally amorphous while the grains in the 100 W film consists 25 % of Si nano-crystallites clusters embedded in an amorphous matrix. The number of grains with size larger than 1 μm is significantly reduced in the film deposited at higher rf power. Grains with the

diameter less than 100 nm is only observed in the films deposited at rf powers of 60 and 80 W but the number is significantly low compared to the larger sized grains. The number of grains with diameter of 100 to 500 nm increases to a maximum with increase in rf power from 20 to 60 W and decreases with further increase in rf power to 100 W. Similar trend is also observed for the grains with diameter of 500 nm to 1 μm but the number increased in the film prepared at rf power of 100 W. The film deposited at rf power of 60 W produces largest number of grains with the diameters in the range of 100 to 500 nm. This film has a crystalline volume fraction of 41 % showing that it is possible for these grains to contain clusters of Si nano-crystallites embedded within an amorphous matrix to produce PL emission as a result of quantum confinement effect.

The FESEM image of a scanned area on the LBL Si:H films deposited at different substrate temperatures is shown in Figure 5.9. The morphology of these films shows similar clusters of Si grains observed in the SEM images of film deposited at different rf powers above 20 W distributed in the scanned area of the films. The sizes of the Si grains appear to be quite uniform and the grains are closely packed and evenly distributed for the film deposited at room temperature. The grain sizes decrease with increase in substrate temperature to 100°C, but the grains are not uniform distributed within the scanned area of the film. The Raman analysis shows an increase in the $X_C$ from 40 to 54 % for the film deposited at room temperature and at substrate temperature of 100°C. With further increase in substrate temperature to 400°C, the grain sizes increase but the clusters are loosely packed resulting lower grain concentration observed. Increase in substrate temperature enhances the local heating and surface mobility for forming larger Si nano-crystallites (Iacona *et al.*, 2000). Raman analysis shows that the $X_C$ decreases to 35 % with increase in substrate temperature to 400°C. The larger grains appear to have lower crystalline volume fraction as compared to the smaller grains. The decrease in H content in the film as a result of increase in substrate

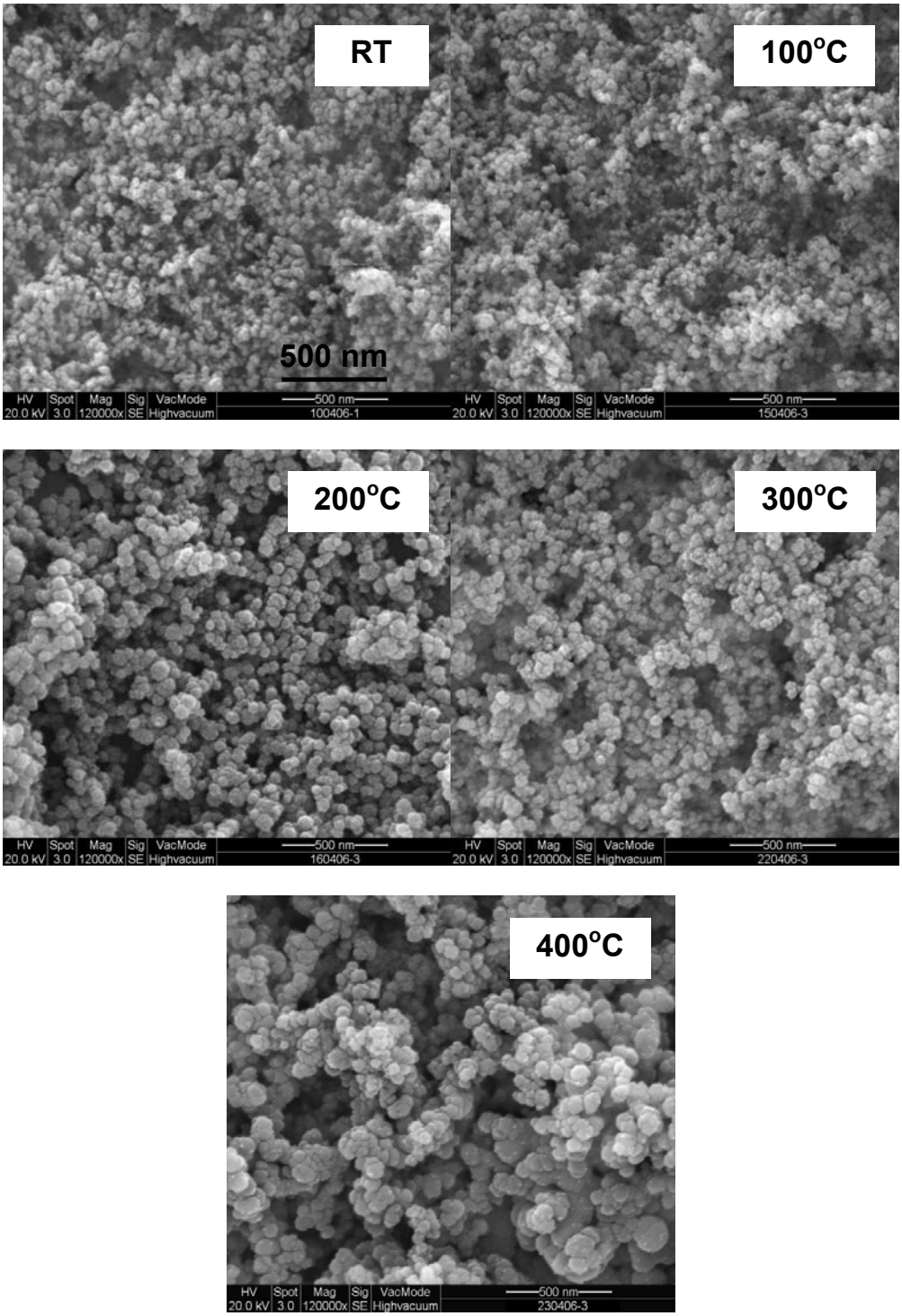


Figure 5.9: FESEM images of the films deposited by LBL deposition technique at different substrate temperatures.

temperature indicated by the FTIR analysis in Chapter 4 also increases the amorphous content in the larger sized grains in LBL deposited films.

Figure 5.10 shows the grain size distribution plot of the films deposited at different substrate temperatures. In the histogram, the grains with the size of less than 10 nm only are present in the SEM images of film deposited at room temperature and substrate temperature of 100°C but the number of grains recorded is very small. The number of grains with the size between 10 to 50 nm increases to a maximum for the film deposited at 100°C and decreases gradually with further increase in substrate temperature. No significant trend is observed for the grains with the size between 50 to 100 nm and above 100 nm. The number of grains with size larger than 100 nm is also small. The $X_C$ appears to have direct relation with the number of grains with the diameter in the range of 10 to 50 nm. Increase in the number of grains of this dimension increases the $X_C$ in the film as a result of variation in the substrate temperature.

### 5.4 Microstructure Study by High Resolution Transmission Electron Microscope

High resolution transmission electron microscope (HRTEM) images of films with evidence of presence of Si nano-crystallites by Micro-Raman scattering spectroscopy are employed to confirm the results. These images are also used to clarify the structure of the Si grains observed from the FESEM images of the films. The HRTEM facility is not available in the University of Malaya during the duration of this PhD work so this HRTEM images (JEOL JEM-3100F, operating at 300 kV) were done using the facility in the Institute of Materials Research and Engineering (IMRE), Singapore. Due to the high cost of performing this characterization, the HRTEM studies were only performed on the LBL films deposited at rf powers of 20, 60 and 100 W. The sample preparation for the TEM measurement was followed by standard sample preparation which is sonication of the film in isopropanol solution and then transfer to

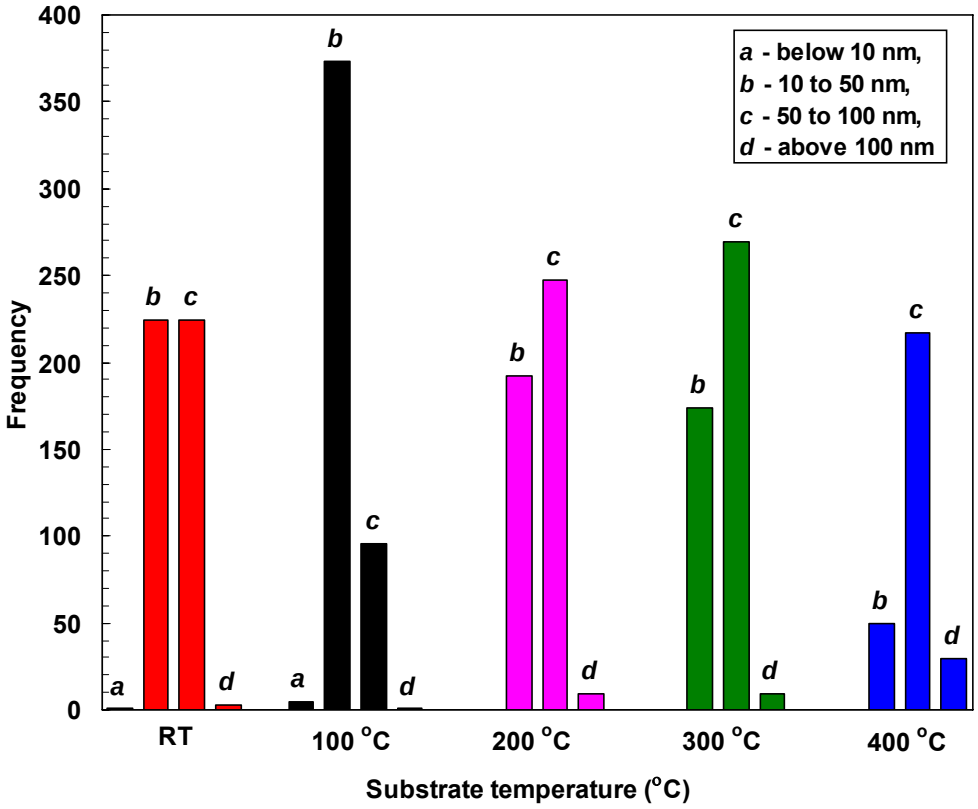


Figure 5.10: Grain size distribution plot for the LBL Si:H films deposited at different substrate temperatures.

copper grid. The sample on the copper grid was kept in the oven at 120°C for 12 hours before the measurement. The HRTEM images of these films are as shown in Figure 5.11. Selected area electron diffraction (SAED) pattern of the Si nano-crystallites observed from the HRTEM image of the film was also obtained using the HRTEM system to further confirm the presence of Si nano-crystallites in the mixed phases of a/nc-Si:H film structure.

The HRTEM images clearly show the presence of clusters of spherical shaped features which is believed to be the Si grains observed in the FESEM images of the films. These spherical shaped features consist of sub-clusters of Si nano-crystallites surrounded by grain boundary of amorphous Si region which hold the nano-crystallites together. The average diameters of these sub-clusters are in the range of 10 to 30 nm. The agglomeration of these sub-clusters forms the grains observed in the FESEM

images of these films. This explains the larger diameters of the Si grains observed from the FESEM images.

Figure 5.11(a) shows the presence of sub-clusters of average diameter 14 nm within the film prepared at low rf power of 20 W. The larger dark spherical regions observed are clusters of these sub-clusters forming the grains observed in the SEM images. The amorphous structure of this film as depicted by the Raman spectrum is confirmed here as the presence of Si nano-crystallites is not evident in this film from the HRTEM image. The HRTEM image of the film prepared at rf power of 60 W shown in Figure 5.11(b) shows that the sub-clusters are larger with average diameter of about 24 nm. Clear presence of Si nano-crystallites embedded within an amorphous matrix in the sub-clusters is evident in the image as shown by the presence of features of periodic arrangements of dots within the sub-clusters. The presence of these crystallites of size less than 3 nm confirms the results obtained from the Raman spectra with peak at 494 $cm^{-1}$. The Raman peak located in the range between 490 $cm^{-1}$ to 504 $cm^{-1}$ has been associated with the presence of very small crystallites of size less than 3 nm surrounded by amorphous grain boundaries (Bi *et al.*, 2006). The presence of these very small crystallites is quite significant from the obvious presence of periodic arrangements of crystal lattices in the HRTEM image. The average diameter of sub-clusters decreases to 20 nm for the film deposited at rf power of 100 W as shown in Figure 5.11(c). However, the crystal lattices in the HRTEM image of the film indicate that the crystallite size is about 4 nm. The rough estimated of the lattice spacing of the crystalline plane from the HRTEM image is about 0.2 which is to correspond to the crystalline silicon (220) plane. The SAED pattern shown in the figure further confirms that the grains observed in the FESEM image of this film prepared at rf powers 100 W consist of sub-clusters of Si nano-crystallites embedded within amorphous matrix. A week spots of crystalline silicon plane of (220) are observed from the SAED image

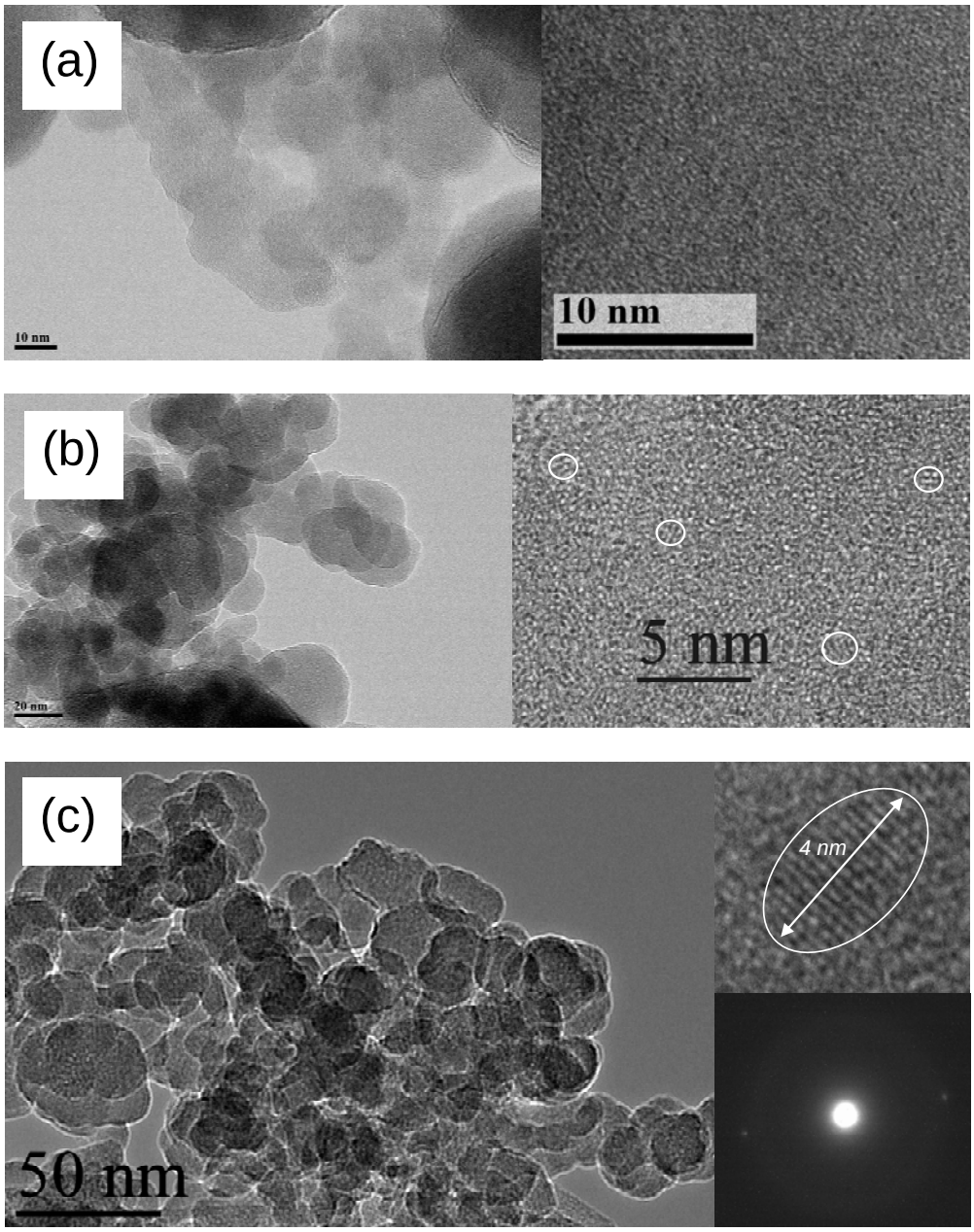


Figure 5.11: HRTEM image of sub-clusters of Si grains obtained from samples deposited at rf powers of (a) 20 W, (b) 60 W and (c) 100 W (Left). Higher magnification HRTEM image in region within the same sub-clusters of the films show the presence of crystalline lattice of nanocrystallites (marked on white circles) embedded within amorphous matrix (Right). Selected area electron diffraction (SAED) pattern (Right bottom) of the nanocrystallites for the sample deposited at rf power of 100 W is also shown.

indicates the preferential growth of crystalline silicon (220) plane. This result is also agreeable with the results obtained from the Raman analysis.

### 5.5 Results and Analysis of Photoluminescence Spectra of Films

Photoluminescence spectroscopy is a very sensitive (contactless and non-destructive) technique for the characterization of optical properties of the films. In this work, the PL emission spectra were obtained using Horiba Jobin Yvon 800 UV Micro-Raman Spectrometer with and CCD detector. The power of laser used was fixed at 20 mW. The excitation wavelength selected was 325 nm HeCd laser and the laser was focused onto a spot of 1 um in diameter to collect the luminescent light from the film after the illumination. The measurement was done at room temperature and atmospheric condition for all the as-deposited films.

Figures 5.12 and 5.13 show the photoluminescence (PL) emission spectra at room temperature as a function of photon energy for the films deposited at different rf powers and $T_s$ respectively. These broad PL emission spectra in the range of 1.2 to 2.8 eV include the visible and infrared regions of the electromagnetic spectrum. Clear evidence of origin of PL in nc-Si:H is still lacking. PL emission at 1.65-1.72 eV has been related to quantum confinement effect due to the presence of nanocrystallites embedded within amorphous matrix by many researchers (Remolina *et al.*, 2009; Mullerova *et al.*, 2006; Trowaga *et al.*, 1998; Kim *et al.*, 2004). On the other hand, higher energy PL emission at 1.86-2.09 eV is associated to defects related to oxygen (Ali *et al.*, 2006). However, the presence of sharp protrusion from the PL emission spectra at energy in range of 1.36-1.41 eV suggests another contribution to the PL of the films studied in this work. Considering the PL emission is at energy lower that the optical energy gap of the films, this emission is associated with radiative recombination of carriers that have been captured by impurities or defects in the films. These PL

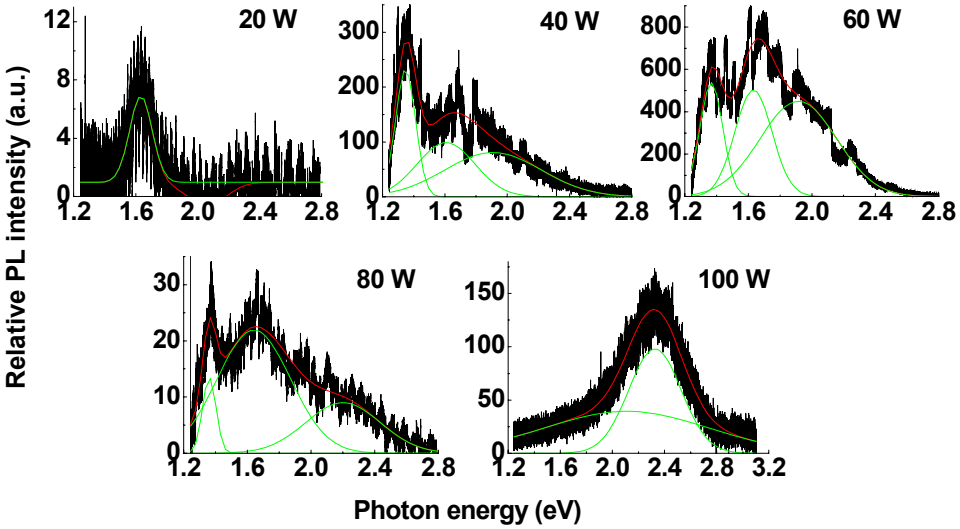


Figure 5.12: Micro-PL spectra of the films deposited by LBL deposition technique at different rf powers.

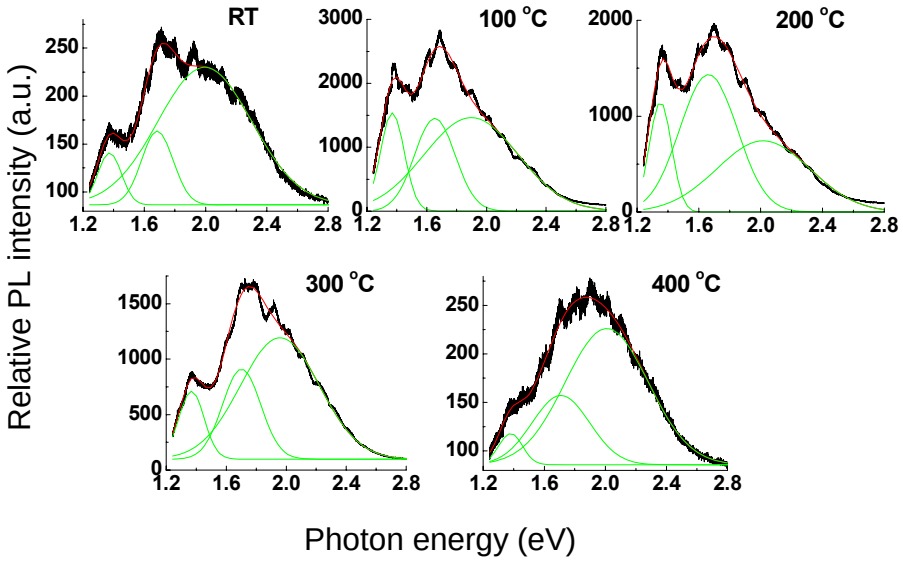


Figure 5.13: Micro-PL spectra of the films deposited by LBL deposition technique at different substrate temperatures, $T_s$.

spectra obtained from these films are decomposed into three components related to the above mentioned origins of PL emission. Gaussian fitting are utilized to deconvolute these spectra into the component peaks and are shown as green colour lines in the figures of PL spectra of the films.

The PL emission spectra of the films deposited at different rf powers is shown in Figure 5.12. The grainy features in the film prepared at rf power of 20 W produces a sharp PL emission spectrum of very low intensity. The amorphous structure of these grains as indicated by the Raman analysis suggests that this emission is due to defects present in the amorphous structure in the film. Prominent broad PL emission spectra are produced by the films deposited at rf powers of 40, 60 and 80 W. The presence of Si nano-crystallites in these films as evident from the Raman results and confirmed by the HRTEM images shows that quantum confinement effects contributes significantly to the PL emission from the grains in these films. PL emission originated from oxygen related defects and structural defects are also present in this film. The intensity of the PL emission spectrum decreases significantly for the films deposited at rf power of 80 W. The analysis on the FESEM image of this film shows that the grain size is comparatively larger than the grain size observed from the other two films and also the density distribution of the grains is lower. This could be the reason for the lower intensity of the PL emission produced by this film. The film deposited at rf power of 100 W produces a narrow PL emission spectrum at 1.8-2.8 eV. This PL emission spectrum is mainly due to oxide contamination at the surface as a result of post-deposition contamination when exposed to air as observed from the FTIR analysis. PL emission related to quantum size effects and defects in the film structure is not observed. The Raman results show that the crystalline volume fraction of the grains in this film is much lower comparatively and the position of crystalline Si peak at 518 $cm^{-1}$ from Raman spectrum also shows that the crystallite size is large for quantum

confinement effect. The intensity of the PL emission for the films deposited at different substrate temperatures are higher compared to the films deposited at different rf powers. The presence of nano-crystallites of size of 3-4 nm with reasonable crystalline volume fraction as shown by the Raman analysis explains presence of PL emission in these films.

Analysis on the PL emission spectra with respect to rf power and substrate temperature are done from the deconvoluted PL spectra into the three component regions detailed in the previous section. The Gaussian fitted components spectra are labelled using a green colour line as shown in Figures 5.12 and 5.13. Fig. 5.14 shows the deconvolution of one of the PL spectrum for clarification on the analysis done in this section on the PL emission data of the films. The component peaks indicated as ***a***, ***b*** and ***c*** correspond to the PL emission in the range of energies of 1.36 – 1.41, 1.65 – 1.72 and 1.86 – 2.09 eV respectively.

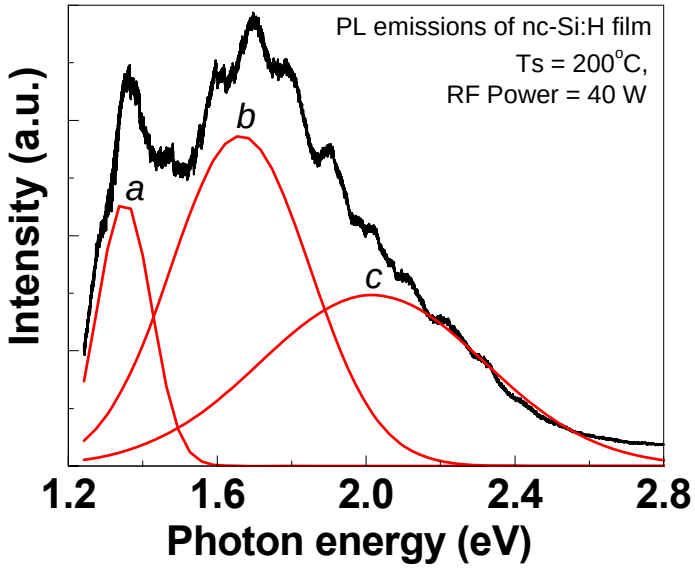


Figure 5.14: Deconvolution of the PL spectra into 3 emission components for the film deposited at substrate temperature of 200°C. The PL emissions indicated as ***a***, ***b*** and ***c*** is correspond to the emission peaks in the range of energies of 1.36 – 1.41, 1.65 – 1.72 and 1.86 – 2.09 eV respectively.

## 5.6 Analysis of Results

*5.6.1 Crystallite Sizes from XRD and Raman Scattering Spectroscopy*

In this section the crystallite sizes as measured from XRD using the Scherrer's equation from the Si (111) and Si (311) orientation planes, the shift of crystalline TO band from c-Si peak in the Raman spectra as described in Section 3.3.4 and HRTEM are analysed and compared.

Figure 5.15 shows the variations of crystallite sizes as measured from the XRD diffraction peaks along the Si (111) and Si (311) planes, and as measured from the shift of the Raman c-Si peak of the samples prepared at different rf powers and substrate temperatures respectively. The crystallite size as measured from the HRTEM images of the samples prepared at rf powers of 60 and 100 W are included in Figure 5.15(a). The nano-crystallites with preferential orientation along the Si (311) plane are larger compared to the nano-crystallites with preferential orientation along the Si (111) plane. It is believed that the former is mostly formed in the lower layers close to the interface as the growth influenced by the seeding layer from lattices in the Si (311) orientation plane of the substrate is most dominant here. The nano-crystallites with preferential

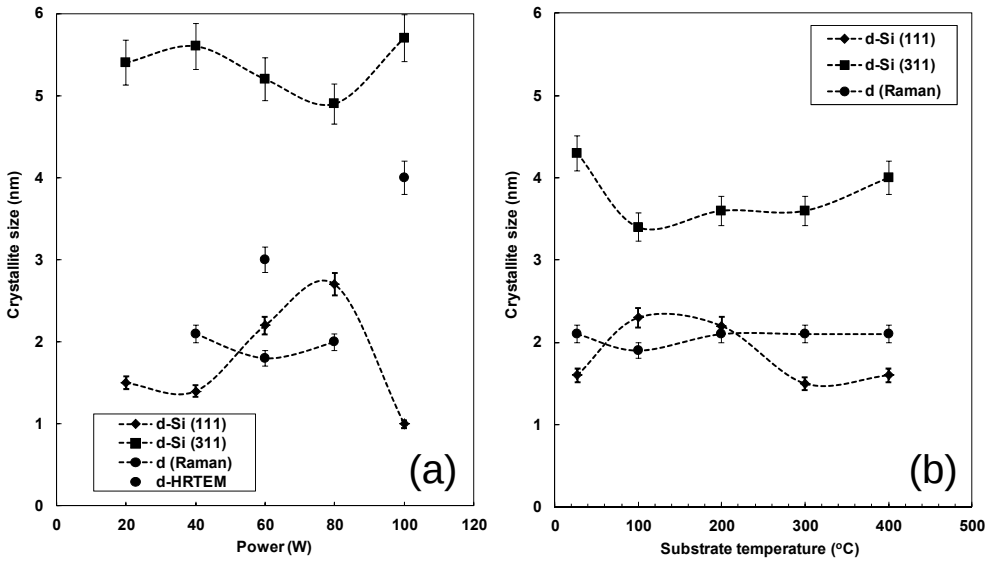


Figure 5.15: Crystallite size with respect to (a) rf power and (b) substrate temperature.

orientation along the Si (111) plane are formed in the upper layers as the growth induced by the seeding layer is reduced. The crystallite sizes measured from the Raman measurements are of the same order as the crystallite size measured for the crystallites with preferential orientation along the Si (111) plane found in the upper layers of the film which consist of mainly of nanocrystaline Si grains. This further confirms that the upper layers consist of Si grains of smaller Si nano-crystallites embedded within an amorphous matrix as the Raman laser penetrates only the upper layers of the sample. The size of the Si nanocrystalline in the HRTEM image in Figure 5.11(c) is almost of the same order as the sizes determined from both the XRD and Raman measurements.

*5.6.2 Crystalline Volume Fraction from XRD and Raman Measurements*

In this work, the crystalline volume fraction is also determined from the XRD diffraction peak along the Si (311) plane. The hydrogen plasma treatment on the c-Si substrate prior to deposition exposes the c-Si (311) lattice to act as seeding layer for nanocrystalline Si film growth. This produces a sharp diffraction peak along the Si (311) plane but the amorphous matrix surrounding the crystallites produces a broad peak overlapping the crystalline diffraction peak. Figure 5.16 shows the de-convolution of this diffraction peak separation the crystalline and amorphous component of the peak. The percentage of the integrated intensity of the crystalline peak to the total integrated intensity of these two diffraction peaks is taken as the crystalline volume fraction of the sample from the substrate to the surface of the LBL deposited samples.

Figure 5.17(a) and (b) compare the crystalline volume fraction as measured from XRD, $X_D$ and Raman measurements, $X_C$ for the samples prepared at different substrate temperatures and rf powers. The results further indicate that the samples deposited by LBL technique form two defined layers consisting of a lower layer of hydrogenated nanocrystalline film above the substrates and an upper layer of aggregates of Si grains

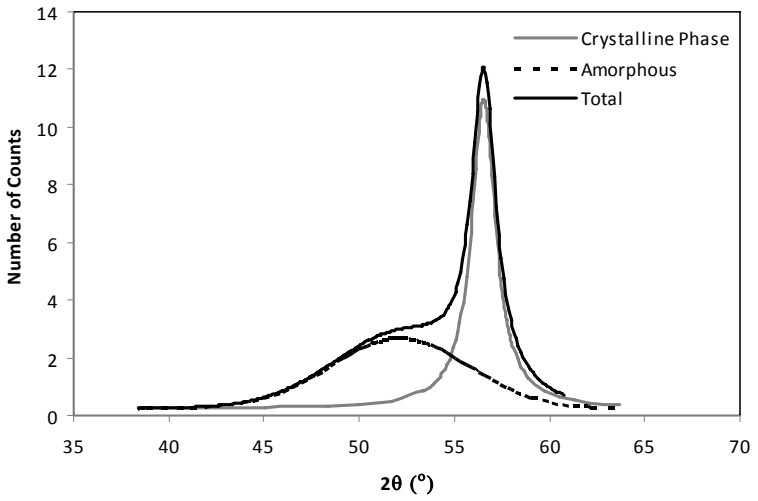


Figure 5.16: De-convolution of the XRD diffraction peak along the Si (311) plane to determine the amorphous and crystalline phase components in the film.

as featured by the SEM images. The crystalline volume fraction measured from the Si (311) diffraction peak includes the lattice induced nanocrystalline Si growth above the substrate and the crystalline Si grains in the upper layers above it while the crystalline volume fraction measured from the Raman peaks only determines the crystalline volume fraction of the Si grain aggregates within the penetration depth of the Raman laser beam.

$X_D$ is generally lower than $X_C$ except for the film deposited at 200°C. On the other hand, the reversed is observed for the films deposited at different rf powers except for the slightly higher $X_C$ compared to $X_D$ for the film prepared at rf power of 40 W. Hydrogen etching effect during the initial hydrogen plasma treatment of the substrates and also during the LBL deposition process is most effective in enhancing the crystallinity of the nanocrystalline Si films on the surface of the substrates especially at high rf powers as indicated by the significantly high $X_D$ compared $X_C$. $X_C$ decreases significantly for the film prepared at rf power of 40 W and does not change much in samples prepared at increasing rf power up to 80W and significantly drops again in the

sample grown at rf power of 100 W. Increase in rf power results in increase in hydrogen etching effects during the hydrogen plasma treatment, increase in dissociation rate of the silane and hydrogen molecules and also increase the ion bombardment effects on the surface of the Si grains. The first two effects increase crystallinity in the Si grains but the last effect destroys crystallinity of the grains. Therefore, the increase in crystallite size in the nanocrystalline grains for the films grown at 40 to 80 W [Figure 5.15(a)] shows that the constant volume fraction in the Si grains in these films is due to increase in the hydrogen etching effect and dissociation rates of the molecules. At low rf power of 20 W, hydrogen etching effect is low but the low dissociation rate increases secondary reaction resulting in more $SiH_3$ radicals reaching the growth surface. This explains the amorphous structure in the film. On the other hand, high ion bombardment effects at rf power of 100 W destroys the crystallinity of the Si grains in the upper layers. Substrate temperature produces almost similar trends on the crystallinity of the nanocrystalline films in the lower layer above the substrates and nanocrystalline Si grains in the upper layers. The increase in crystallite size in the Si grains in the upper

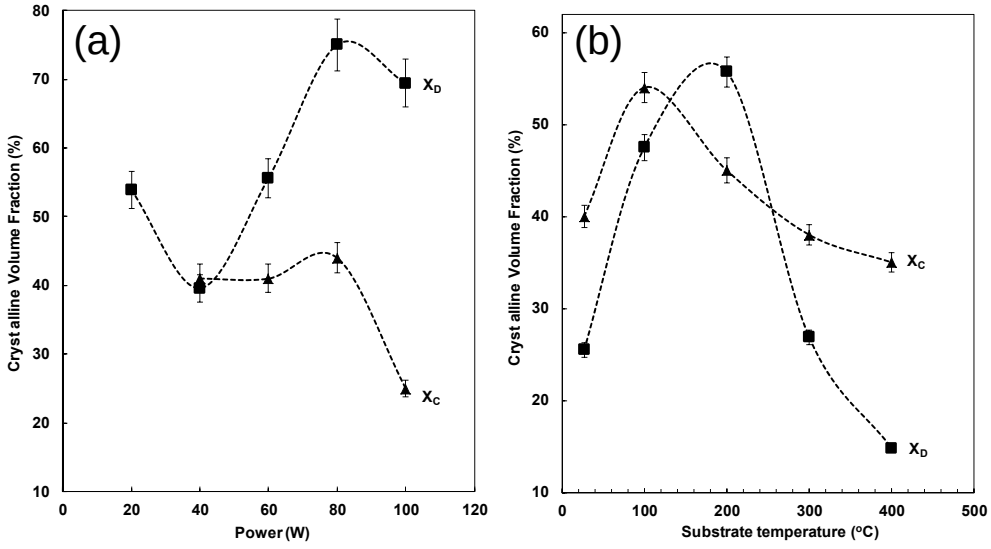


Figure 5.17: Crystalline volume fraction as measured from Raman and XRD measurements with respect to (a) rf power and (b) substrate temperature.

layers and decrease in crystallite size in the lower layers for samples prepared at rf power of 100 and 200°C appear to enhance the crystallinity of the lower nc-Si film as well as the nanocrystalline grains in the upper layers. At these temperatures, $SiH_3$ growth radicals and H atoms are effectively diffused into the Si grains in the upper layers as well as the nc-Si films in the lower layers to enhance the crystallinity in both layers.

*5.6.3 Effects of RF Power and Substrate Temperature on PL Intensity*

Figure 5.18(a) shows the plot of PL emission intensity as a function of substrate temperature. The PL emission intensity for the film deposited at 100°C is the highest and the emission mainly contributed by the presence of oxides and Si related defects in the Si grains are most dominant. These PL intensities decrease sharply with increase in substrate temperature. The PL emission in the range of 1.65 to 1.72 eV believed to be contributed by quantum confinement effect in the nanocrystalline Si grains showed lower intensity but is consistently high for the films deposited at 100, 200 and 300°C. Similarly, this PL emission intensity dropped significantly for the film deposited at substrate temperature of 400°C. The PL emissions for the films deposited at different rf powers as shown in Figure 5.18(b) are generally lower than the films deposited at different substrate temperatures. This is because these films are deposited at substrate temperature of 300°C which as shown in Figure 5.18(a) that high substrate temperature lowers the PL intensity of the sample deposited by LBL technique. However, the PL intensity emitted by the film deposited at rf power of 60 W is the highest and the emission contributed by quantum confinement effect in the nanocrystalline Si grains is most dominant. The emission contributed by oxygen related defects is least dominant. The trends with respect to rf power are similar for all emissions. The results also shows crystalline volume fraction of the crystalline grains is an important parameter

influencing the PL intensity of the LBL deposited samples. The films showing high $X_C$ consistently emit high PL emission thus showing the PL emission from the LBL samples are emitted from the nc-Si grains in the upper layers.

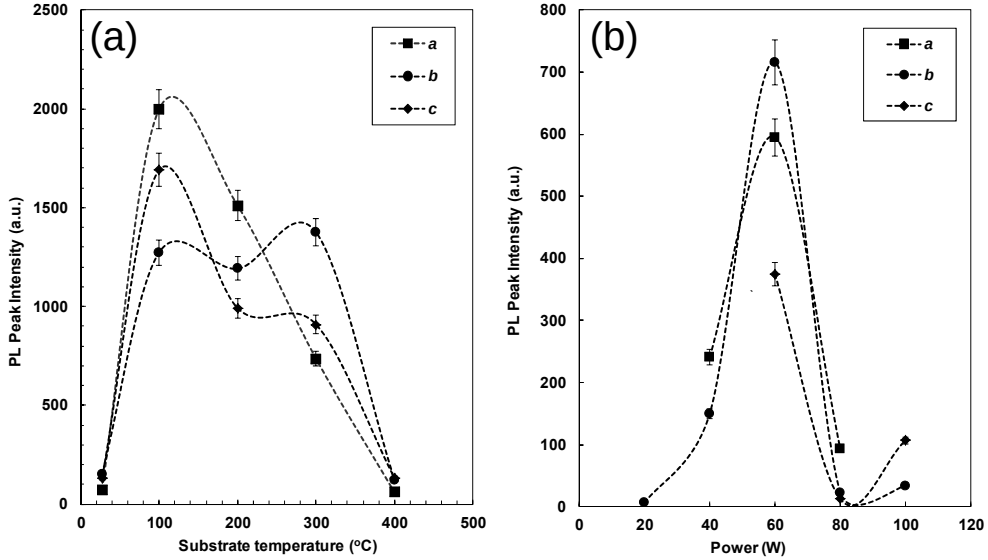


Figure 5.18: Variation of PL intensity with (a) substrate temperature and (b) rf power.

*5.6.4 Effects of RF Power and Substrate Temperature on PL Peak Position*

Figure 5.19(a) and (b) show the variation of PL emission energy indicated by the peak position with respect to substrate temperature and rf power respectively. The crystallite sizes determined from the XRD diffraction peak along the Si (111) plane which represent the crystallite size of the Si nano-crystallites in the Si grains in the upper layers are also included in these figures. The crystallite sizes with respect to substrate temperature show reversed trends with the variation of PL peak positions for emissions at *b* and *c* which are due to quantum confinement effects and oxygen related defects respectively. Increase in the crystallite size decreases the PL emission energy and vice-versa. This property indicates that these two emissions are related to quantum confinement effects in the Si grains. This shows that the Si nano-crystallites in these films are embedded in mixed phases of a-Si and amorphous silicon oxide (a-SiO)

matrix and the proportion of these phases in the grain boundary are dependent on the substrate temperature. Figure 5.19(b) shows that emission related to quantum confinement effects is only indicated by the emission *b*. This shows that only this emission is related to quantum confinement effect in the nc-Si grains prepared at different rf powers showing that the Si nano-crystallites are embedded in a-Si matrix only. This explains why PL emission intensity at 1.65 – 1.72 eV is most dominant at all rf power particularly for the film prepared at rf power of 60 W.

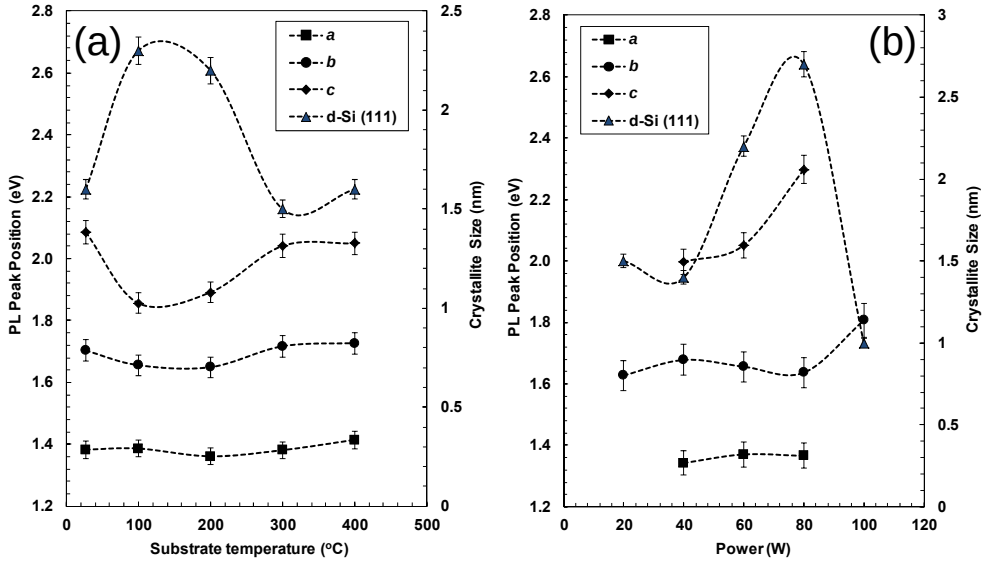


Figure 5.19: Variation of PL emission energy represented by the peak position with (a) substrate temperature and (b) rf power.

*5.6.5 Influence of Oxygen Content on PL Emission Intensity*

The results above show that the crystallinity and crystallite sizes play an important role in the PL emission properties of the films as PL emission due quantum confinement effects is most dominant in these LBL deposited samples. Also PL emission in these samples is shown to be produced by the n-Si grains in the upper layers. However, the results show that PL intensity is highest when the amorphous matrix comprises of mixed phases of a-Si and a-SiO matrix. In this section, the significance of the presence of SiO phase in the nc-Si grains on the PL emission

intensity is investigated. Figure 5.20(a) and (b) show the variation of Si-O stretching band peak position and integrated intensity versus substrate temperature and rf power respectively. These results are obtained from the FTIR spectra of the LBL films presented in Chapter 4. It is observed that Si-O bonds are present in all the films although the precursor gas used are silane and hydrogen. The oxygen atoms forming these bonds are believed to be either diffused from the virgin oxide layer on the substrates during deposition or diffused through dangling bond passivation after the deposition process when the Si grains are exposed to air. The peak position of Si-O stretching band at 1082 $cm^{-1}$ for the film deposited at room temperature indicates that the oxide formed is close to stoichiometric $SiO_2$. This film also has significantly high integrated intensity for the Si-O stretching band indicating high concentration of these bonds in the film. This oxide is believed to be formed at the interface prior to deposition of the film as hydrogen etching process done prior to deposition at room temperature on the surface of the c-Si substrate is not energetic enough to weaken the Si-O bonds at the surface for diffusion into the Si grains in the upper layers. Probability of post-deposition oxygenation of the Si grains is also very low at this substrate temperature since the availability of dangling bonds is low when the film is exposed to air. The peak position shows a significant shift towards lower wave-numbers and the integrated intensity also dropped drastically with increase in substrate temperature. The hydrogen plasma treatment on the heated substrate surface weakens the Si-O bonds at the surface and during the deposition process these oxygen atoms are diffused onto the Si grains within the amorphous grain boundaries separating the Si nano-crystallites. The heated substrates increase the diffusion rate of the O atoms into the upper layers. Repeated hydrogen plasma treatments diffuse more oxygen atoms into the Si grains but at high substrate temperature, oxygen atoms diffused to the upper layers are evolved. Oxygen atoms are also diffused onto the Si grains when exposed to air after deposition as

oxygen atoms passivate available dangling bonds especially in films with low H contents. However, the concentration of Si-O bonds is significantly decreased with increase in substrate temperature especially for the samples deposited at 300 and 400°C indicating only a small amount is diffused into the grain boundaries of the Si grains making them more Si rich at high substrate temperature. The high PL emission produced by the film prepared at 100°C suggests that the a-SiO component is important in enhancing the PL emission intensity of the film. The low PL intensity of the film deposited at room temperature despite of having high content of oxygen atoms is believed to be due to the fact that the oxygen atoms in the films are mostly concentrated at the interface and not in the amorphous matrix of the Si grains. The low PL intensity of the film deposited at 300 and 400°C shows that quantum confinement effects is low for these films as the amorphous grain boundary surrounding the nano-crystallites has very low oxygen content which is important in enhancing the energy gap. This also explains the lower PL intensities of the films prepared at different rf powers as these films were deposited at high substrate temperature of 300°C. The low oxygen content in these films also results in the low PL emission of these films. The PL emission is also shown to be mainly contributed by quantum confinement effect in nc-Si grains and not oxygen related defect. The PL emission originated from oxygen related defects also shows that the PL emission at these samples is not due to quantum confinement effect as indicated by the relation of the PL peak position with crystallite size in Figure 5.19(b). The significant increase in the Si-O band integrated intensity for the film prepared at rf power of 100 W is still not significant enough to increase the PL intensity as compared to the film prepared at substrate temperature of 100°C. The results strongly indicate the presence of the a-SiO phase in the grain boundaries of the nc-Si grains contribute to the enhancement of PL emission.

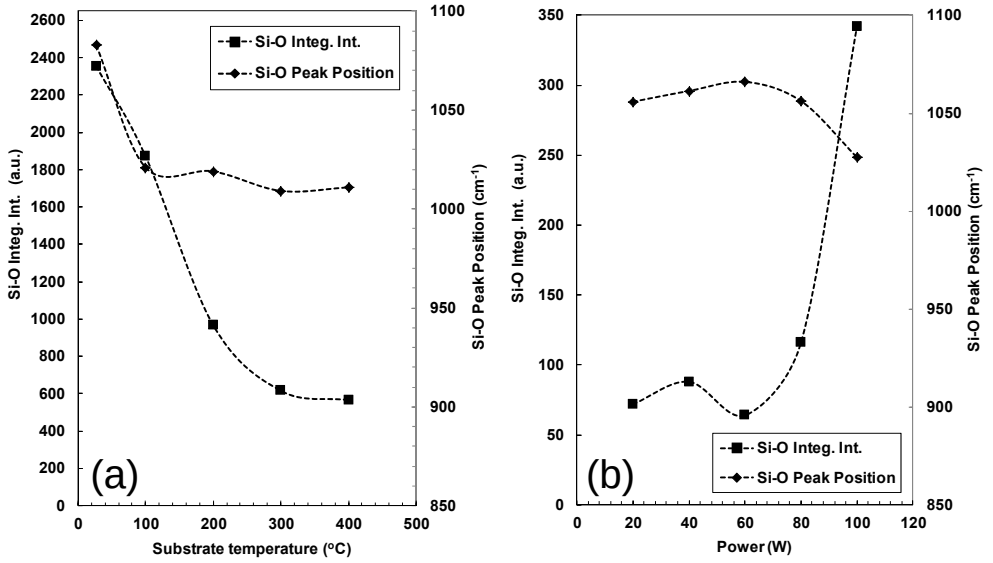


Figure 5.20: Variation of Si-O stretching band integrated intensity and peak position with (a) substrate temperature and (b) rf power.

## 5.7 Proposed Growth Mechanism of Nanocrystalline Silicon Grains with Photoluminescence Emission Properties by LBL Deposition

Figure 5.21 outlines the proposed growth mechanism of aggregates of nc-Si:H grains on c-Si (111) substrates by LBL deposition using PECVD technique. These nc-Si:H grains are favourably grown at low substrate temperatures of 100 and 200°C and exhibit room temperature PL emission. The ten minutes hydrogen plasma treatment on the c-Si substrate prior to deposition done at the same deposition conditions as the Si layers weakens Si-O bonds on the surface [Figure 5.21(a)]. These Si-O bonds are formed when the c-Si substrates are exposed to air prior to insertion into the deposition chamber. The hydrogen plasma treatment at substrate temperatures of 100 and 200°C only weakens these bonds, however if done at higher temperatures these oxygen atoms are evolved from the substrates leaving Si dangling bonds. During the discharge of $SiH_4$ and $H_2$ molecules cycle, growth radicals consisting mainly of $SiH_3$ radicals and reactive H atoms reach the substrate surface [Figure 5.21(b)]. These radicals are produced through dissociation of $SiH_4$ and secondary reactions of these radicals with excess $SiH_4$ and also $H_2$ molecules. Surface reactions at the growth sites mainly through abstraction

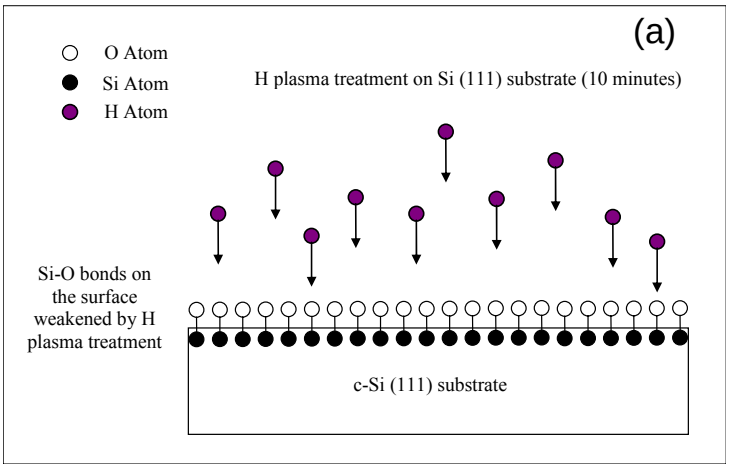


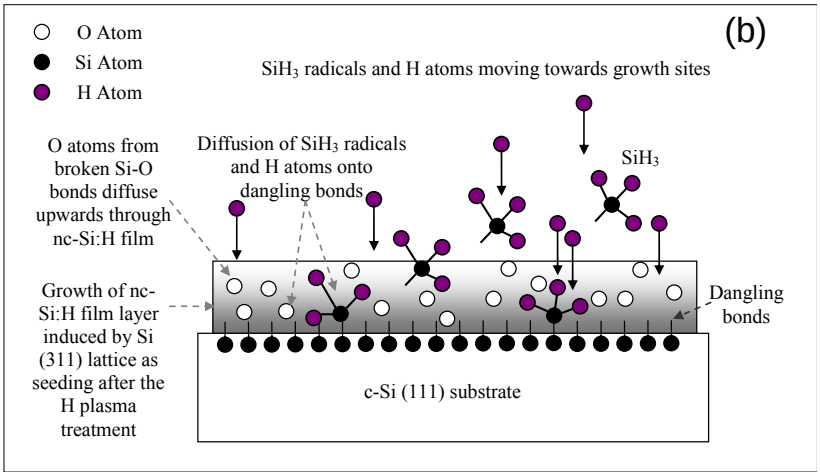


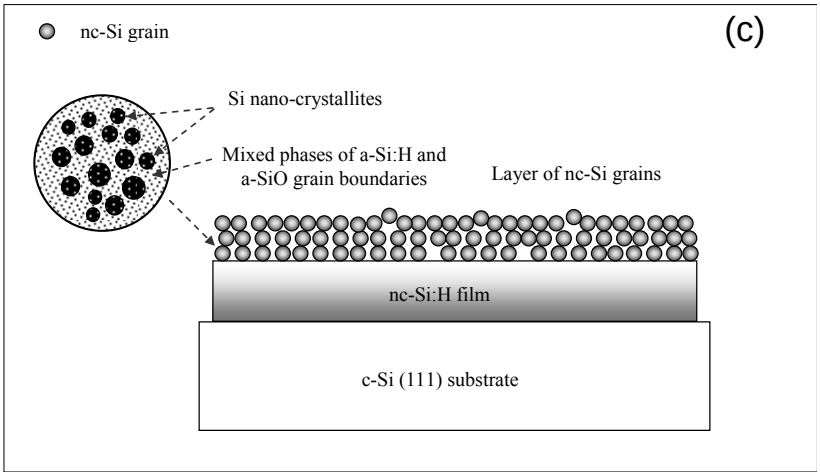


Figure 5.21: Proposed deposition mechanism of nc-Si:H grains with PL emission properties by LBL deposition: (a) Hydrogen plasma treatment on the c-Si substrate surface done prior to deposition weakens Si-O bonds at the surface and exposes Si (311) lattices which act as seeding layer for the lower layer of nc-Si:H film. (b) Diffusion of O atoms from broken Si-O bonds upwards through the nc-SiH film formed as a result of LBL deposition process. (c) The formation of aggregates of nc-Si:H grains on the nc-Si:H film layer above the c-Si substrate. The proposed structure of the nanocrystalline Si grain is shown to consist of Si nano-crystallites embedded within mixed phases of a-Si:H and a-SiO matrix.

and diffusion process of $SiH_3$ radicals results in the growth of nc-Si:H films on the substrates. The growth of the earlier layers is induced by the Si (311) lattice exposed by the hydrogen plasma treatment. These lattices acts as seeding layers for the growth of the nc-Si:H film with preferred orientation along the Si (311) plane. The thermal energy produced by the heating of the substrates breaks the weakened Si-O bonds and diffuses the O atoms upwards through the nc-Si:H film layer. When the effect of the seeding layer of the c-Si lattice diminishes as the nc-Si:H layer increases in thickness, nc-Si:H grains are formed and some of the O atoms at the surface that has diffused to the surface of the nc-Si:H layer are absorbed into the amorphous matrix of the grains. The following cycles of the hydrogen plasma treatment of the LBL process removes weak Si-Si bonds and forms Si nano-crystallites embedded in mixed phases of a-Si:H and a-SiO matrix. These nano-crystallites are much smaller than the ones in the film in the lower layers and have preferred orientation in the Si (111) orientation plane. Figure 5.21(c) shows the resultant layer of nc-Si:H film formed in the lower layer above the substrate and the aggregates of nc-Si:H grains formed above the nc-Si:H film. The presence of a-SiO phase in the grain boundaries enhances quantum confinement effects and the formation of highly crystalline grains produced high intensity PL emission at room temperature. The PL emission covers a wide range in the visible spectrum.

## 5.8 Summary

In this chapter, the results of the effects of rf power and substrate temperature on the crystallinity, surface morphology, microstructure and photoluminescence properties of nc-Si grains for the Si:H films deposited by LBL deposition technique have been discussed and studied.

The Raman spectra of the films deposited at rf powers of 40 to 100 W showed that the Si grains consisted of clusters of Si nano-crystallites surrounded by grain

boundaries. The low hydrogen etching effect during the LBL deposition process at low rf power resulted in the formation of amorphous Si grains. The crystalline volume fraction decreased with increase in substrate temperature due to increase in the size of the clusters of Si nano-crystallites resulting in the increase in the number and size of voids in between the clusters which are filled with amorphous Si phase.

The crystallinity of the films extracted from the XRD in Chapter 4 showed that the Si nano-crystallites with preferential orientation along the Si (311) plane were formed in the lower layers close to the interface of the film and substrate. At the surface of the substrate, Si (311) lattice acted as seeding layers for the growth. Si nano-crystallites with preferential orientation along the Si (111) plane were formed in the upper layers as a result of the hydrogen plasma treatment. These nano-crystallites were clustered together and were embedded within the amorphous matrix forming nc-Si grains. Hydrogen etching effects effectively enhanced the crystallinity in the lower and upper layers of the nc-Si films especially at high rf powers. The films prepared at rf powers of 100 and 200°C showed the crystallinity was enhanced with increase in the crystallite size of the Si nano-crystallites in the upper layers but decrease in crystallite size in the lower layer near the surface of the substrate.

The FESEM images showed that the films consisted of nc-Si grains with clusters of Si nano-crystallites surrounded by grain boundaries embedded in amorphous Si matrix. These Si grains were either randomly or evenly distributed on the film surface depending on the deposition conditions. Films deposited at low substrate temperature of 100°C had the largest number of grains with the diameters in the range of 10 to 50 nm and showed the highest crystalline volume fraction of 54%. The crystalline volume fraction appeared be enhanced with the presence of small diameter of grains with 10 to 50 nm.

The HRTEM images confirmed the presence of clusters of spherical shaped features with Si nano-crystallites embedded in an amorphous matrix in the sub-cluster. The films deposited at rf powers of 40 and 60 W, substrate temperatures of 100, 200 and 300°C, produced high intensity of PL emissions in a wide range of photon energy between 1.2 to 2.8 eV at room temperature. The presence of Si nano-crystallites in the nc-Si grains in these films contributed significantly to the PL emissions at 1.65 to 1.72 eV which was due to the quantum confinement effects. However, the presence of oxygen related defects and structural defects in the Si matrix were shown to be responsible for the PL emissions at 1.86-2.09 and 1.36-1.41 eV respectively. The results showed that the PL emission intensities of the films strongly depended on the deposition conditions, and the crystalline volume fraction and crystallite size were shown to determine the PL emission properties of the nc-Si grains. The results also showed that these Si nano-crystallites in the films were embedded in mixed phases of a-Si and amorphous silicon oxide (a-SiO) matrix. The proportion of these phases in the grain boundary was dependent on the deposition conditions and presence of the a-SiO phase in the grain boundaries of the nc-Si grains contributed to the enhancement of PL emission.

The PL emission intensities of the films have been correlated to the crystalline volume fraction and the inverse of crystallite size. The higher crystalline volume fraction resulted in higher PL integrated intensity resulting from the quantum confinement effect. However, the PL emission diminished with the decrease of the crystallite size which approached amorphous structure, resulting in the disappearance of quantum confinement effect. The PL emissions due to oxygen related defects and structural defects in the Si matrix were only present when PL emission due to quantum confinement effect was present. This showed that the oxygen related defects and Si-Si

structural defects which were believed to be centres for PL emission were related to the nanostructures present in films.

Finally, the growth mechanism of nc-Si grains has been proposed to explain the photoluminescence emission properties for the deposited films by LBL deposition technique at different deposition conditions.